

Climate Dynamics

The Influence of Ocean Dynamics on the Tropical Atlantic SST Bias in CESM1

--Manuscript Draft--

| | |
|--|---|
| Manuscript Number: | |
| Full Title: | The Influence of Ocean Dynamics on the Tropical Atlantic SST Bias in CESM1 |
| Article Type: | Original Article |
| Keywords: | Tropical Atlantic SST bias; CESM1; CCSM4 |
| Corresponding Author: | Sang-ki Lee, Ph.D. CIMAS Miami, FL UNITED STATES |
| Corresponding Author Secondary Information: | |
| Corresponding Author's Institution: | CIMAS |
| Corresponding Author's Secondary Institution: | |
| First Author: | Zhenya Song, Ph.D. |
| First Author Secondary Information: | |
| Order of Authors: | Zhenya Song, Ph.D. Sang-ki Lee, Ph.D. Chunzai Wang, Ph.D. Benjamin Kirtman, Ph.D. Fangli Qiao, Ph.D. |
| Order of Authors Secondary Information: | |
| Abstract: | <p>In order to identify and quantify inherent errors in the atmosphere-land model and the ocean-sea ice model components of the Community Earth System Model version 1 (CESM1), and their contributions to the tropical Atlantic sea surface temperature (SST) bias in CESM1, we propose a new method of diagnosis and apply it to a series of CESM1 simulations. Our analysis of the model simulations indicates that the ocean-sea ice model contributes significantly to the eastern equatorial Atlantic warm SST bias in CESM1 due to its spurious ocean dynamic processes. Therefore, while we acknowledge the potential importance of the westerly wind bias in the western equatorial Atlantic and the low-level stratus cloud bias in the southeastern tropical Atlantic, both of which originate from the atmosphere-land model, we emphasize here that solving those problems in the atmosphere-land model alone does not resolve the equatorial Atlantic warm bias in CESM1.</p> |
| Suggested Reviewers: | <p>Ingo Richter richter@jamstec.go.jp Dr. Richter published multiple papers about tropical Atlantic bias in CMIP3 and CMIP5 models.</p> <p>Shang-Ping Xie sxie@ucsd.edu Dr. Sang-Ping Xie published multiple papers about tropical Atlantic bias in CMIP3 and CMIP5 models.</p> <p>Zeng-Zhen Hu Zeng-Zhen.Hu@noaa.gov Dr. Hu has published multiple papers on the tropical Atlantic bias in CFS</p> <p>Bohua Huang huangb@cola.iges.org Dr. Huang published multiple papers on tropical Atlantic SST bias in CFS.</p> |

1 **The Influence of Ocean Dynamics on the Tropical Atlantic SST Bias**
2 **in CESM1**

3
4
5
6
7
8

9 Zhenya Song^{1,2,3}, Sang-Ki Lee^{1,2}, Chunzai Wang², Ben Kirtman⁴ and Fangli Qiao³

10 ¹Cooperative Institute for Marine and Atmospheric Studies, University of Miami, Miami FL

11 ²Atlantic Oceanographic and Meteorological Laboratory, NOAA, Miami FL

12 ³First Institute of Oceanography, State Oceanic Administration, Qingdao China

13 ⁴Rosenstiel School of Marine and Atmospheric Sciences, University of Miami, Miami, Florida

14
15
16
17
18
19
20
21

Submitted to Climate Dynamics

January 2014

22 Corresponding author address: Dr. Sang-Ki Lee, CIMAS, University of Miami, 4600
23 Rickenbacker Causeway, Miami, FL 33149, USA. E-mail: Sang-Ki.Lee@noaa.gov.

24
25
26
27
28
29
30
31
32
33
34
35
36
37
38
39
40
41
42
43
44
45
46

Abstract

In order to identify and quantify inherent errors in the atmosphere-land model and the ocean-sea ice model components of the Community Earth System Model version 1 (CESM1), and their contributions to the tropical Atlantic sea surface temperature (SST) bias in CESM1, we propose a new method of diagnosis and apply it to a series of CESM1 simulations. Our analysis of the model simulations indicates that the ocean-sea ice model contributes significantly to the eastern equatorial Atlantic warm SST bias in CESM1 due to its spurious ocean dynamic processes. Therefore, while we acknowledge the potential importance of the westerly wind bias in the western equatorial Atlantic and the low-level stratus cloud bias in the southeastern tropical Atlantic, both of which originate from the atmosphere-land model, we emphasize here that solving those problems in the atmosphere-land model alone does not resolve the equatorial Atlantic warm bias in CESM1.

47 **1. Introduction**

48 Since the pioneering work of Manabe and Bryan (1969), coupled atmosphere-ocean general
49 circulation models (AOGCMs) have significantly improved. AOGCMs are now able to
50 reproduce the basic features of the global climate system (Covey et al. 2003; Meehl et al. 2005),
51 and thus become an important tool for seasonal forecasts, climate projections and other climate
52 research in general.

53 However, the tropical Atlantic biases typically characterized by warmer sea surface
54 temperatures (SSTs) in the eastern equatorial ocean, a reversed zonal SST gradient along the
55 equator, colder SSTs in the northwest and southwest tropical Atlantic, and warmer SSTs in the
56 northeast and southeast tropical Atlantic, are common problems with most AOGCMs (e.g.,
57 Davey et al. 2002).

58 Model biases have been somewhat reduced in most recent models used in the Coupled Model
59 Intercomparison Project Phase 5 (CMIP5) compared to those used in CMIP3 (e.g., Liu et al.
60 2013). Recent studies have also shown that improving the spatial resolution can potentially
61 reduce such biases (Gent et al. 2010; Patricola et al. 2011; Kirtman et al. 2012). Nevertheless,
62 almost all of the state-of-the-art AOGCMs still cannot reproduce the climatology of tropical
63 Atlantic SSTs (Mechoso et al. 1995; Davey et al. 2002; Covey et al. 2003; Richter and Xie 2008;
64 Richter et al. 2012).

65 These systematic tropical Atlantic biases in AOGCMs will affect the models' ability to
66 simulate and predict climate variability (Xie and Carton 2004). Studies have shown that the
67 tropical Atlantic affects and modulates climate variability of the Western Hemisphere, such as
68 the West African summer monsoon (Vizy and Cook 2001; Giannini et al. 2003; Gu and Adler
69 2004), moisture transport and rainfall over the American continents (Enfield et al. 2001; Wang et

70 al. 2006) and Atlantic hurricane development and intensification (e.g., Goldenberg et al. 2001;
71 Webster et al. 2005; Wang and Lee 2007). Therefore, in order to increase the seasonal-to-decadal
72 climate predictability in the Western Hemisphere, it is important to accurately simulate the
73 tropical Atlantic Ocean in AOGCMs.

74 Many studies have diagnosed the large systematic errors in the tropical Atlantic, and
75 attributed the errors to various atmospheric and/or ocean processes. Recent studies argued that
76 the westerly wind bias over the western tropical Atlantic in boreal spring is the main cause of the
77 tropical Atlantic biases (Richter and Xie 2008; Richter et al. 2012), and showed that the westerly
78 wind bias also exists in the atmosphere general circulation models (AGCMs) forced by observed
79 SSTs (DeWitt 2005; Chang et al. 2007; Richter and Xie 2008; Richter et al. 2012). These studies
80 argued that the westerly wind bias in boreal spring deepens the thermocline in the eastern
81 equatorial Atlantic and prevents the development of the cold tongue in summer; then warm SST
82 bias develops in the cold tongue and further amplifies due to the Bjerknes feedback.

83 Other studies have suggested that a likely source of the tropical Atlantic biases is the
84 deficiency of AOGCMs in reproducing the low-level stratus cloud deck over the southeastern
85 tropical Atlantic Ocean (Yu and Mechoso 1999; Large and Danabasoglu 2006; Saha et al. 2006;
86 Huang et al. 2007; Hu et al. 2008; 2011; Richter and Xie 2008). These studies argue that the
87 warm SST bias over the southeastern tropical Atlantic is mainly caused by the model's inability
88 to reproduce the observed amount of low-level cloud in the region, which in turn causes an
89 excessive local shortwave radiative flux into the ocean. Wahl et al. (2011) explored this
90 hypothesis by performing some sensitivity experiments using the Kiel Climate model. Wahl et
91 al. (2011) concluded that the westerly wind bias over the western tropical Atlantic in spring and
92 early summer is the key mechanism for the equatorial Atlantic SST bias, while the low-level

93 cloud cover and associated excessive surface shortwave radiation contribute to the SST bias in
94 the southeast tropical Atlantic Ocean.

95 There are also some studies suggesting that ocean processes could contribute to the tropical
96 Atlantic biases. Hazeleger and Haarsma (2005), for example, suggested that the tropical Atlantic
97 bias is strongly related to the upper ocean mixing. Seo et al. (2006) argued that properly
98 representing equatorial Atlantic instability waves in climate models could enhance the equatorial
99 upwelling and thus potentially reduce the equatorial Atlantic warm SST bias. Large and
100 Danabasoglu (2006) suggested that the warm SST bias in the southeastern tropical Atlantic could
101 be reduced by improving the simulation of coastal upwelling off the coasts of southwest Africa.
102 Breugem et al. (2008) attributed the warm SST bias in the eastern and southeastern tropical
103 Atlantic to the spurious barrier layer (BL), which forms due to the excessive regional rainfall and
104 amplifies via coupled SST-precipitation-BL feedback and thus prevents surface cooling via
105 strong salinity stratification. However, Richter et al. (2012) showed that the BL feedback
106 described by Breugem et al. (2008) is not significant at least in the Geophysical Fluid Dynamics
107 Laboratory (GFDL) coupled model. There are also other interesting hypotheses on the origin of
108 the tropical Atlantic SST bias in the coupled models, such as the meridional SST dipole (Lee and
109 Wang 2008; Chang et al. 2007), the West African monsoon (Deser et al. 2006), rainfall over the
110 Amazon and Africa (Davey et al. 2002; Chang et al. 2008; Okumura and Xie 2004), and air-sea
111 turbulent flux (Ban et al. 2010).

112 Previous studies such as those briefly reviewed above have suggested a variety of potential
113 causes of the tropical Atlantic SST biases in AOGCMs. However, these hypotheses (or
114 conclusions) are derived largely based on fully spun up AOGCM runs. Since the SST bias in an
115 AOGCM could cause errors in the atmospheric circulation, which in turn also could feedback

116 onto the tropical Atlantic SSTs via air-sea interaction, it is almost impossible to identify the exact
117 processes responsible for the tropical Atlantic SST bias from fully spun up AOGCM runs.
118 Therefore, in an effort to identify the exact processes that cause the tropical Atlantic SST biases,
119 here we focus on the initial development of the SST bias by using the National Center for
120 Atmospheric Research (NCAR) Community Earth System Model version 1 (CESM1), which
121 suffers the same systematic tropical Atlantic SST bias as in other AOGCMs.

122 This paper is organized as follows. The model and numerical experiments design are
123 described in section 2. The experiment results and analysis are presented in section 3 and 4, in
124 which the SST bias and its development mechanism in CESM1 are analyzed by comparing
125 results from three model experiments (to be described in section 2). Section 5 provides
126 conclusions and discussion.

127

128 **2. Model and model experiments**

129 CESM1 is a state-of-the-art global earth system model that can provide simulations of the
130 Earth's past, present, and future climate. It is the successor to the Community Climate System
131 Model (CCSM), which was extended and renamed to CESM in June 2010. CESM1, which was
132 released in November 2012, is a superset of CCSM4 in that its default configuration is the same
133 science scenarios as CCSM4, although CESM1 also contains options for a terrestrial carbon
134 cycle and dynamics, and ocean ecosystems and biogeochemical coupling, all necessary for an
135 earth system model. In this paper, CESM1 is configured as a purely physical model, and is thus
136 identical to CCSM4, since our focus here is on the physical processes. Many improvements have
137 been made in CESM1/CCSM4 simulations compared with the previous version of CCSM3, such
138 as the frequency of the Madden - Julian Oscillation (MJO) and ENSO variability, the annual

139 cycle of SSTs in the eastern equatorial Pacific, and the Arctic sea-ice concentration (Gent et al.
140 2011). However, it still displays significant tropical Atlantic SST biases (Grotsky et al. 2012) as
141 shown in Figure 1b. The observed SSTs in the equatorial Atlantic are warmer in the west and
142 cooler in the east (Figure 1a). However, the SSTs in the CCSM4 control simulation with
143 twentieth century forcing (CCSM4_20C hereafter), which is available from the CMIP5 archive,
144 are warmer in the east and cooler in the west with the SST bias exceeding 3.0°C in the southeast
145 tropical Atlantic along the east coast of Africa (Figure 1b). It is clear that CCSM4_20C fails to
146 reproduce the equatorial Atlantic cold tongue and the zonal SST gradient along the equator,
147 which are common deficiencies in AOGCMs.

148 The main objective of this study is to identify the processes responsible for the development
149 of the tropical Atlantic SST biases in CESM1. Our approach to achieve this goal is to diagnose
150 the development of biases in a fully coupled CESM1 run initialized with data from uncoupled
151 surface-forced atmosphere and ocean only simulations. It is worthwhile to point out that this
152 approach is analogous to the one used in the Transpose-Atmospheric Model Intercomparison
153 Project Phase II (T-AMIP2) as discussed in Williams et al. (2013).

154 Three numerical experiments are designed and performed using CESM1. These experiments
155 are (1) dynamic atmosphere-land run forced by observed SSTs (EXP_ATM hereafter); (2)
156 dynamic ocean-sea ice run forced by observed surface atmospheric fluxes (EXP_OCN
157 hereafter); and (3) fully coupled atmosphere-land-ocean-sea ice run initialized with data from
158 EXP_ATM and EXP_OCN (EXP_CPL hereafter).

159 The atmosphere model component is Community Atmosphere Model version 4 (CAM4;
160 Neale et al. 2010) and the land model is Community Land Model version 4 (CLM4; Lawrence et
161 al. 2011). Both CAM4 and CLM4 have horizontal resolution of $1.9^\circ \times 2.5^\circ$, and are forced by

162 observed climatological monthly SSTs (Hurrell et al. 2008). This experiment (EXP_ATM) is
 163 integrated for 30 years and the last ten years are used for analysis. The ocean model is Parallel
 164 Ocean Program version 2 (POP2; Danabasoglu et al. 2012) and the sea-ice model is Community
 165 Ice Model version 4 (CICE4; Hunke and Lipscomb 2008). Both POP2 and CICE4 have a
 166 nominal 1° horizontal resolution, and are forced by Coordinated Ocean Reference Experiment
 167 phase 2 (COREv2) normal-year surface fluxes (Large and Yeager 2004; 2009). This experiment
 168 (EXP_OCN) is integrated for 210 years and the last ten years are used for analysis.

169 For the fully coupled experiment (EXP_CPL), 10-member ensemble experiments are
 170 performed to achieve statistically significant model results. The atmosphere and surface land
 171 models are initialized using EXP_ATM while the ocean and sea-ice models are initialized using
 172 EXP_OCN. The 10-member ensemble experiments are initialized using the combination of the
 173 EXP_ATM and EXP_OCN obtained from the last 10 years of the model integrations, and
 174 integrated for five years. In the following sections, the ensemble-mean of EXP_CPL along with
 175 the results from EXP_ATM and EXP_OCN are analyzed to identify the processes that cause the
 176 development of the tropical Atlantic SST biases in CESM1.

177

178 **3. Implicit SST bias in EXP_ATM and EXP_OCN**

179 3.1 EXP_ATM

180 In order to understand and quantify the roles of the atmospheric-land model (EXP_ATM) in the
 181 generation of the tropical Atlantic SST bias, the net surface heat flux bias in EXP_ATM is
 182 integrated in time:

$$183 \quad \Delta T_{\text{EXP_ATM}}(t) = \int_0^t \frac{Q_{\text{NET}}[\text{EXP_ATM}] - Q_{\text{NET}}[\text{OBS}]}{\rho_w C_{pw} D} dt, \quad (1)$$

184 where ρ_w is sea water density, C_{pw} is the specific heat of sea water, D is the mixed layer depth
185 from EXP_OCN, $Q_{NET}[EXP_ATM]$ and $Q_{NET}[OBS]$ are the net surface heat fluxes from
186 EXP_ATM and COREv2, respectively. Note that ΔT_{EXP_ATM} represents SST bias, which could be
187 potentially caused by the net surface heat flux bias for the duration of t , with assumptions that the
188 atmosphere-land model is coupled with a perfect ocean (i.e., all oceanic heat flux terms are error-
189 free) and there is no air-sea feedback to amplify or damp out the net surface heat flux bias.
190 Obviously, the net heat flux bias in this case (EXP_ATM) does not change the model SSTs
191 because the model SSTs are fixed. Therefore, it is referred to as *implicit SST bias* in EXP_ATM,
192 hereafter.

193 Figure 2a shows the annually averaged implicit SST bias in EXP_ATM due to the net surface
194 heat flux bias. This is computed by integrating the long-term averaged net heat flux bias in
195 EXP_ATM from January 1 to December 31, then dividing it by 12 months. Using a similar
196 method, the annually averaged implicit SST bias in EXP_ATM due to the latent heat flux,
197 shortwave radiative heat flux, and longwave radiative heat flux, are computed and shown in Fig.
198 2b, c, and d, respectively. As shown in Fig. 2a, the north-central equatorial Atlantic and also the
199 southeastern tropical Atlantic between 20°S and the equator are characterized by warm (implicit)
200 SST bias; while in other regions, especially in the south and north tropical Atlantic, there are two
201 bands of cold (implicit) SST bias across the Atlantic basin. These results suggest that if the
202 atmosphere-land model is coupled with a perfect ocean and the SST bias does not feedback onto
203 the atmosphere-land model, warm SST bias is expected in the north-central equatorial Atlantic
204 and the southeastern tropical Atlantic, whereas cold SST bias is expected in the north and south
205 tropical Atlantic.

206 Figure 2c shows that the warm/cold implicit SST biases in EXP_ATM are mainly caused by
207 weaker/stronger surface wind stress bias and associated positive (i.e., into the ocean)/negative
208 (i.e., out of the ocean) latent heat flux bias. As shown in Fig. 2b, the shortwave radiative flux is
209 larger than observations over the stratus cloud deck region of the south-central and southeastern
210 tropical Atlantic Ocean, south of around 10°S (Large and Danabasoglu 2006; Huang et al. 2007;
211 Grodsky et al. 2012). Although not shown here, CCSM4_20C also contains the positive
212 shortwave radiative flux bias in the southeastern tropical Atlantic with about the same amplitude
213 of that in EXP_ATM, suggesting that the low-level cloud and shortwave radiation errors in
214 CCSM4_20C are inherent to its atmospheric-land component. However, Figure 2d shows that
215 the positive shortwave radiation flux bias in the southeastern tropical Atlantic is partly
216 compensated by the negative long wave radiative heat flux bias in the region. Therefore, the net
217 radiative flux bias in EXP_ATM has a relatively weak influence on the implicit SST bias in the
218 southeastern tropical Atlantic (not shown).

219

220 3.2 EXP_OCN

221 Figure 3 shows the SST bias in the surface-forced ocean-sea ice model experiment (EXP_OCN).
222 Overall, the tropical Atlantic SSTs are reasonably well simulated with a relatively low amplitude
223 of SST bias. Nevertheless, the amplitude of warm SST bias in the southeastern tropical Atlantic
224 especially near the west coast of Africa is quite large (up to 2°C). This suggests that inherent
225 errors in the ocean-sea ice model can significantly contribute to the warm SST bias in
226 CCSM4_20C, in agreement with earlier studies (Large and Danabasoglu 2006; Grodsky et al.
227 2012).

228 It is important to note that in EXP_OCN the ocean-sea ice model is forced with prescribed
 229 atmospheric conditions. Flux forms of atmospheric forcing, namely short and longwave radiative
 230 heat fluxes, precipitation rate and wind stress are directly used to force the ocean-sea ice model.
 231 For latent and sensible heat fluxes, however, bulk equations are used to compute them
 232 interactively using wind speed, air humidity and air temperature at 10 m along with the model
 233 SSTs. Such a treatment of the turbulent heat fluxes ultimately relaxes the model SSTs toward the
 234 prescribed surface air temperature as discussed in earlier studies (e.g., Lee et al. 2007; Liu et al.
 235 2012). Therefore, the SST bias in EXP_OCN shown in Fig. 3 is not a good measure of inherent
 236 errors in the ocean-sea ice model.

237 To better quantify the inherent errors in EXP_OCN, we attempt to compute implicit SST bias
 238 in EXP_OCN associated with spurious ocean dynamic processes. The equation for the surface
 239 mixed layer temperature bias in EXP_OCN can be written as

$$240 \quad \frac{\partial \Delta T_m}{\partial t} = -\Delta \left(u_m \frac{\partial T_m}{\partial x} + v_m \frac{\partial T_m}{\partial y} + w_e (T_m - T_e) \right) + \frac{Q_{NET} [\text{EXP_OCN}] - Q_{NET} [\text{OBS}]}{\rho_w C_{pw} D}, \quad (2)$$

241 where ΔT_m is the difference in ocean mixed layer temperature between EXP_OCN and the
 242 observation, u_m and v_m are the ocean mixed layer currents in the x - and y -directions, w_e is the
 243 entrainment rate at the mixed layer base, T_e is the ocean temperature immediately below the
 244 mixed layer, and $Q_{NET} [\text{EXP_OCN}]$ is the net surface heat flux in EXP_OCN (see Lee et al. 2007
 245 for the derivation of the bulk mixed layer temperature equation). The first three terms on the
 246 right side of equation (2) can be regarded as the errors in ocean dynamic processes. Integrating
 247 equation (2) in time, after a minor manipulation, we get

$$\begin{aligned}
\Delta T_{\text{EXP_OCN}} &\equiv -\int_0^t \Delta \left(u_m \frac{\partial T_m}{\partial x} + v_m \frac{\partial T_m}{\partial y} + w_e (T_m - T_e) \right) dt \\
&= \Delta T_m - \int_0^t \frac{Q_{\text{NET}}[\text{EXP_OCN}] - Q_{\text{NET}}[\text{OBS}]}{\rho_w C_{pw} D} dt.
\end{aligned}
\tag{3}$$

248 $\Delta T_{\text{EXP_OCN}}$ represents the implicit SST bias in EXP_OCN due to the inherent errors in the ocean
250 dynamic processes, including advection and turbulent mixing, for the duration of t with
251 assumptions that there is no air-sea feedback to amplify or damp out the net surface heat flux
252 bias.

253 Figure 4a shows the annually averaged implicit SST bias in EXP_OCN linked to spurious
254 ocean dynamic processes. Its amplitude is of the same order of magnitude as that in EXP_ATM
255 (Fig. 2a). Comparing Fig. 4a with Fig. 2a, in the southeastern and northeastern tropical Atlantic,
256 especially near the west coast of Africa, the implicit SST bias due to spurious ocean dynamic
257 processes is much larger than that due to net heat flux bias in EXP_ATM. This strongly suggests
258 that the warm SST biases in CCSM4_20C over these regions (see Fig. 1b) are mainly associated
259 with spurious ocean dynamic processes.

260 It is interesting to note that ocean dynamic cooling in EXP_OCN is too strong in the eastern
261 equatorial Atlantic, but too weak in the central equatorial Atlantic. Given that vertical
262 entrainment of cold thermocline water due to turbulent mixing is what maintains the cold tongue
263 in the central equatorial Atlantic (e.g., Lee and Csanady 1999a; 1999b; Goes and Wainer 2003),
264 it is possible that the parameterization of vertical mixing, and/or the mean state variables that
265 affect the vertical mixing, namely vertical shear and stratification at the mixed layer base, are the
266 source of the SST bias. It is also possible that failing to resolve equatorial Atlantic instability
267 waves reduces the equatorial upwelling and is thus responsible for the warm implicit SST bias in
268 the central equatorial Atlantic (Seo et al. 2006).

269

270 3.3 EXP_ATM + EXP_OCN

271 The linear combination of the implicit SST bias in EXP_ATM due to net surface heat flux bias
272 (1) and the implicit SST bias in EXP_OCN due to spurious ocean dynamic processes (3) can be
273 written as

$$274 \quad \Delta T_{\text{EXP_ATM}} + \Delta T_{\text{EXP_OCN}} = \Delta T_m + \int_0^t \frac{Q_{\text{NET}}[\text{EXP_ATM}] - Q_{\text{NET}}[\text{EXP_OCN}]}{\rho_w C_{pw} D} dt. \quad (4)$$

275 This SST bias is what is expected when the atmosphere-land model is joined together with the
276 ocean-sea ice model but without any air-sea feedback. It is important to note that the implicit
277 SST bias in EXP_ATM + EXP_OCN is independent from the observed surface heat flux product
278 used in the analysis, and is thus not subject to uncertainty in the observed surface heat flux
279 product used at least in a linear sense.

280 Figure 4b shows the implicit SST bias in EXP_ATM + EXP_OCN. Comparing this with the
281 SST bias in CCSM4_20C (Fig. 1b), their spatial patterns are surprisingly similar although the
282 overall amplitude of SST bias in CCSM4_20C is smaller than the amplitude of implicit SST bias
283 in EXP_ATM + EXP_OCN. In particular, in both CCSM4_20C and EXP_ATM + EXP_OCN,
284 the southwestern and northwestern tropical Atlantic are characterized by cold SST bias, while the
285 southeastern and northeastern tropical Atlantic are characterized by warm SST bias. This result
286 mainly suggests that the cold/warm SST biases over these off-equatorial regions in CCSM4_20C
287 originate from the inherent biases in the atmosphere-land model and the ocean-sea ice model,
288 and further weakened/amplified by atmosphere-ocean coupling.

289 However, it appears that over the equatorial Atlantic region the implicit SST bias in
290 EXP_ATM + EXP_OCN (Fig. 4b) does not exactly explain the SST bias in CCSM4_20C (Fig.
291 1b). Therefore, to better understand the origin of the equatorial Atlantic SST bias in

292 CCSM4_20C, in the next section we explore the initial development of the tropical Atlantic SST
293 bias in EXP_CPL.

294

295 **4. Initial development of the SST bias in EXP_CPL**

296 Figure 4c shows the SST bias in EXP_CPL averaged over the first year. Overall, both the
297 amplitude and spatial pattern of the SST bias in EXP_CPL developed over the first year are very
298 similar to those of the annually averaged SST bias in CCSM4_20C (Fig. 1b), suggesting that the
299 tropical Atlantic SST bias develops very quickly. Figure 5 shows the bi-monthly SST bias
300 development in the fully coupled model experiment (EXP_CPL) during the first and second
301 years of the model integration.

302 An interesting point is that the cold SST bias in the eastern equatorial Atlantic, which
303 apparently originates from the ocean-sea ice model (Fig. 4a), persists only during the first four
304 months of the coupled model integration. However, it disappears afterward and is completely
305 masked by the warm SST bias in June of the first year. Among other features, perhaps the most
306 striking is the fast development of the warm SST bias in the southeastern tropical Atlantic - the
307 SST bias along the coast of Angola exceeds 6°C by June of the first year.

308 Although the tropical Atlantic SST bias in EXP_CPL develops very quickly within a year,
309 largely due to the combined effect of inherent biases in EXP_ATM and EXP_OCN, in some
310 regions the SST bias in the first year is further weakened or amplified due to the active
311 atmosphere-ocean coupling. For instance, the cold SST bias over the southwestern tropical
312 Atlantic in the first year is much reduced in the second year due to the eastward expansion of the
313 warm SST anomalies in the southeastern tropical Atlantic. It is also clear that the warm SST bias

314 in the eastern equatorial Atlantic during the first year strengthens and expands westward in the
315 second year.

316 In order to better describe the tropical SST biases in EXP_CPL and how they are forced by
317 EXP_ATM, EXP_OCN and the atmosphere-ocean coupling, the bi-monthly tropical Atlantic
318 SST bias tendencies ($^{\circ}\text{C month}^{-1}$) in EXP_CPL, EXP_ATM + EXP_OCN, EXP_ATM and
319 EXP_OCN during the first year are shown in Fig. 6. It is clearly shown that the southeastern
320 tropical Atlantic warm SST bias in EXP_CPL, which is largely forced in boreal spring, is caused
321 by EXP_OCN due to spurious ocean dynamic processes, with an assumption that the surface
322 fluxes prescribed in EXP_OCN is error-free. The initial development of the eastern equatorial
323 warm SST bias, which is mainly forced in early boreal summer, is also caused by EXP_OCN due
324 to spurious ocean dynamic processes.

325 By comparing the SST bias tendency in EXP_CPL and the implicit SST bias tendency in
326 EXP_OCN, it is clear that the atmosphere-ocean coupling tends to weaken the implicit SST bias
327 tendency in these regions, and thus does not play a decisive role at least in the first year. These
328 features in the equatorial Atlantic are much more clearly illustrated in Fig. 7, which shows the
329 time evolutions of the SST bias tendencies along the equatorial Atlantic and the contributions by
330 the surface heat flux errors and by errors involving ocean dynamic processes in EXP_CPL.
331 Therefore, we may conclude that the eastern equatorial and southeastern tropical Atlantic warm
332 SST biases in EXP_CPL are forced by EXP_OCN due to its spurious ocean dynamic processes.

333 Richter and Xie (2008) analyzed CMIP3 models and argued that the westerly wind bias in
334 boreal spring over the western equatorial Atlantic deepens the thermocline in the eastern
335 equatorial Atlantic preventing the development of the cold tongue in summer, and thus is the root
336 cause of the equatorial Atlantic warm SST bias in CMIP3 models. Our analysis of the three

337 CESM1 experiments, however, suggests that the ocean-sea ice model due to its spurious ocean
338 dynamic processes may contribute more significantly than the atmosphere-land model to the
339 eastern equatorial Atlantic warm SST bias in CCSM4/CESM1. Therefore, while we
340 acknowledge the potential importance of the westerly wind bias in boreal spring over the western
341 equatorial Atlantic, which originates from the atmosphere-land model (see Fig. 2b), we would
342 like to stress that solving this problem in the atmosphere-land model alone does not resolve the
343 equatorial Atlantic warm bias in CCSM4/CESM1.

344 Grodsky et al. (2012) showed that mean sea level pressure in CCSM4 is erroneously high by
345 a few millibars in the subtropical highs and erroneously low in the polar lows similar to CCSM3,
346 and thus the trade winds are $1 \sim 2 \text{ m s}^{-1}$ too strong. Since the cold SST biases in the southwestern
347 and northwestern tropical Atlantic are closely linked to the strength of the trade winds in
348 EXP_ATM, it is likely that their root cause is the subtropical highs in the atmosphere-land
349 model.

350

351 **5. Summary and Discussions**

352 In order to identify the processes that contribute significantly to the initial development of the
353 tropical Atlantic SST bias in AOGCMs, we have performed a series of model experiments using
354 CESM1. These experiments are a forced atmosphere-land model experiment (EXP_ATM), a
355 forced ocean-ice model experiment (EXP_OCN) and a fully coupled model experiment with its
356 atmosphere-land model initialized using EXP_ATM and the ocean-ice model using EXP_OCN
357 (EXP_CPL).

358 We propose and use a new method of diagnosis to identify and quantify inherent errors in the
359 atmosphere-land model and the ocean-sea ice model components of CESM1. It is shown here

360 that both the atmosphere-land model and the ocean-sea ice model components contain significant
361 errors in the tropical Atlantic. In particular, in boreal summer, the ocean-sea ice model could
362 cause large amplitudes of warm SST bias in the eastern equatorial and southeastern tropical
363 Atlantic due to its spurious ocean dynamic processes even if it is coupled to a perfect
364 atmosphere-land model and the SST bias does not feedback onto the ocean-sea ice model. In the
365 atmosphere-land model, the trade winds and associated surface latent cooling are too strong in
366 the northwestern and southwestern tropical Atlantic, while they are too weak in the northeastern
367 and southeastern tropical Atlantic. Therefore, even if the atmosphere-land model is coupled to a
368 perfect ocean-sea ice model and the SST bias does not feedback onto the atmosphere-land
369 model, warm SST bias could be generated in the northeastern and southeastern tropical Atlantic,
370 whereas cold SST bias could be generated in the northwestern and southwestern tropical
371 Atlantic.

372 In the fully coupled model simulation with its atmosphere-land model initialized using
373 EXP_ATM and the ocean-sea ice model using EXP_OCN, the tropical Atlantic SST bias
374 develops very quickly within a year, and its amplitude and spatial pattern are largely determined
375 by the linear combination of the implicit SST errors in EXP_ATM and EXP_OCN. In particular,
376 it is shown here that the eastern equatorial and southeastern tropical Atlantic warm SST bias in
377 the fully coupled simulation are forced in boreal spring and early summer by the ocean-sea ice
378 model due to its spurious ocean dynamic processes, and further grow due to positive atmosphere-
379 ocean feedback.

380 We point out that our results are not entirely independent from uncertainty in the observed
381 surface flux product used (i.e., COREv2). In particular, if the observed surface zonal wind is too
382 weak along the equator, it will contribute positively to the equatorial Atlantic warm SST bias in

383 EXP_OCN. Although considerable effort was made to minimize errors, COREv2 is far from
384 perfect. Therefore, in a more strict sense, equation (3) should be considered as the implicit SST
385 bias in EXP_OCN and COREv2. Similarly, equation (1) should be considered as the implicit
386 SST bias in EXP_ATM and COREv2.

387 The main emphasis in this paper is to explore how the tropical SST bias in CESM1 is
388 initiated and evolves. Although we identify that the inherent errors in the ocean-sea ice model
389 contribute significantly to the tropical SST bias in CESM1, further studies are needed to trace the
390 parameterizations and/or configurations in the ocean-sea ice model that are directly linked to the
391 errors. Therefore, we strongly recommend sensitivity studies on model resolutions (in both the
392 horizontal and vertical directions), vertical mixing schemes and isopycnal mixing schemes, using
393 the ocean-sea ice model component of CESM1.

394

395 **Acknowledgments.** We would like to thank Marlos Goes and Libby Johns for their useful
396 comments. This research was supported by National Science Foundation Grant ATM-0850897,
397 International Cooperation Project of Ministry of Science and Technology of China
398 2011DFA20970, the Public Science and Technology Research Funds Projects of Ocean
399 201105019, and the base funding of NOAA Atlantic Oceanographic and Meteorological
400 Laboratory (AOML). All model simulations used in this study were carried out at National
401 Supercomputer Center in Tianjin, China.

402

403 **References**

404 Ban J, Gao Z, Lenschow DH (2010) Climate simulations with a new air-sea turbulent flux
405 parameterization in the National Center for Atmospheric Research Community Atmosphere
406 Model (CAM3). *J Geophys Res* 115:D01106. doi:10.1029/2009JD012802

407 Breugem W-P, Chang P, Jang CJ, Mignot J, Hazeleger W (2008) Barrier layers and tropical
408 Atlantic SST biases in coupled GCMs. *Tellus A* 60:885-897. doi:10.1111/j.1600-
409 0870.2008.00343.x

410 Chang C-Y, Carton JA, Grodsky SA, Nigam S (2007) Seasonal climate of the tropical Atlantic
411 sector in the NCAR Community Climate System Model 3: error structure and probable
412 causes of errors. *J Clim* 20: 1053–1070

413 Chang C-Y, Nigam S, Carton JA (2008) Origin of the springtime westerly bias in equatorial
414 Atlantic surface winds in the Community Atmosphere Model version 3 (CAM3) simulation.
415 *J Clim*, 21:4766-4778

416 Covey C, AchutaRao KM, Cubasch U, Jones P, Lambert SJ, Mann ME, Phillips TJ, Taylor KE
417 (2003) An overview of results from the Coupled Model Intercomparison Project. *Global*
418 *Planet Change* 37:103-133

419 Danabasoglu G, Bates SC, Briegleb BP, Jayne SR, Jochum M, Large WG, Peacock S, Yeager
420 SG (2012) The CCSM4 Ocean Component. *J Clim*, 25:1361–1389. doi:
421 <http://dx.doi.org/10.1175/JCLI-D-11-00091.1>

422 Davey M, and coauthors (2002): STOIC: a study of coupled model climatology and variability in
423 tropical ocean regions. *Clim Dyn* 18:403-420

424 Deser C, Capotondi A, Saravana R, Phillips AS (2006) Tropical Pacific and Atlantic climate
425 variability in CCSM3. *J Clim* 19:2451-2481

426 DeWitt DG (2005) Diagnosis of the tropical Atlantic near-equatorial SST bias in a directly
427 coupled atmosphere-ocean general circulation model. *Geophys Res Lett* 32:L01703.
428 doi:10.1029/2004GL021707

429 Enfield DB, Mestas-Nuñez AM, Trimble PJ (2001) The Atlantic multidecadal oscillation and its
430 relation to rainfall and river flows in the continental US. *Geophys Res Lett* 28:2077-2080

431 Gent PR, Yeager SG, Neale RB, Levis S, Bailey DA (2010) Improvements in a half degree
432 atmosphere/land version of the CCSM. *Clim Dyn* 34:819-833

433 Gent PR, and coauthors (2011) The community climate system model version 4. *J Clim* 24:4973-
434 4991

435 Giannini A, Saravanan R, Chang P (2003) Oceanic forcing of Sahel rainfall on interannual to
436 interdecadal time scales. *Science* 302:1027-1030

437 Goes M, Wainer I (2003) Equatorial currents transport changes for extreme warm and cold
438 events in the Atlantic Ocean. *Geophys Res Lett* 30: 8006, doi:10.1029/2002GL015707

439 Goldenberg SB, Landsea CW, Mestas-Nuñez AM, Gray WM (2001) The recent increase in
440 Atlantic hurricane activity: Causes and implications. *Science* 293:474-479

441 Grodsky SA, Carton JA, Nigam S, Okumura YM (2012) Tropical Atlantic biases in CCSM4, *J*
442 *Clim* 25:3684-3701. doi: <http://dx.doi.org/10.1175/JCLI-D-11-00315.1>

443 Gu G, Adler RF (2004) Seasonal evolution and variability associated with the West African
444 monsoon system. *J Clim* 17:3364-3377

445 Hazeleger W, Haarsma RJ (2005) Sensitivity of tropical Atlantic climate to mixing in a coupled
446 ocean-atmosphere model. *Clim Dyn* 25:387-399

447 Hu Z-Z, Huang B, Pegion K (2008) Low cloud errors over the southeastern Atlantic in the NCEP
448 CFS and their association with lower-tropospheric stability and air-sea interaction. *J Geophys*
449 *Res* 113:D12114. doi:10.1029/2007JD009514

450 Hu Z-Z, Huang B, Hou Y-T, Wang W, Yang F, Stan C, Schneider EK (2011) Sensitivity of
451 tropical climate to low-level clouds in the NCEP climate forecast system. *Clim Dyn* 36:1795-
452 1811

453 Huang B, Hu Z-Z, Jha B (2007) Evolution of model systematic errors in the tropical Atlantic
454 basin from coupled climate hindcasts. *Clim Dyn* 28:661-682

455 Hunke EC, Lipscomb WH (2008) CICE: The Los Alamos sea ice model user's manual, version
456 4. Los Alamos National Laboratory Tech Rep, LA-CC-06-012, 76pp

457 Hurrell JW, Hack JJ, Shea D, Caron JM, Rosinski J (2008) A new sea surface temperature and
458 sea ice boundary dataset for the Community Atmosphere Model. *J Clim* 21:5145-5153

459 Kirtman BP, and coauthors (2012) Impact of ocean model resolution on CCSM climate
460 simulations. *Clim Dyn* 39:1303-1328

461 Large WG, Danabasoglu G (2006) Attribution and impacts of upper-ocean biases in CCSM3. *J*
462 *Clim* 19:2325–2346. doi: <http://dx.doi.org/10.1175/JCLI3740.1>

463 Large WG, Yeager SG (2004) Diurnal to decadal global forcing for ocean and sea ice models:
464 the data sets and climatologies. NCAR Tech. Note 460+STR, 105 pp

465 Large WG, Yeager SG (2009) The global climatology of an interannually varying air–sea flux
466 data set. *Clim Dyn* 33:341-364. doi:10.1007/s00382-008-0441-3

467 Lawrence DM, and coauthors (2011) Parameterization improvements and functional and
468 structural advances in version 4 of the Community Land Model. *J Adv Model Earth Syst*
469 3:M03001. doi:10.1029/2011MS000045

470 Lee S-K, Csanady GT (1999a) Warm water formation and escape in the upper tropical Atlantic
471 Ocean: 1. A literature review. *J Geophys Res* 104:29561-29571. doi:10.1029/1999JC900079.

472 Lee S-K, Csanady GT (1999b) Warm water formation and escape in the upper tropical Atlantic
473 Ocean: 2. A numerical model study. *J Geophys Res* 104:29573–29590.
474 doi:10.1029/1999JC900078.

475 Lee S-K, Enfield DB, Wang C (2007) What drives the seasonal onset and decay of the Western
476 Hemisphere warm pool? *J Clim* 20:2133-2146

477 Lee S-K, Wang C (2008) Tropical Atlantic decadal oscillation and its potential impact on the
478 equatorial atmosphere–ocean dynamics: A simple model study. *J Phys Oceanogr* 38:193–
479 212. doi: <http://dx.doi.org/10.1175/2007JPO3450.1>

480 Liu H, Wang C, Lee S-K, Enfield DB (2013) Atlantic warm pool variability in the CMIP5
481 simulations. *J Clim* 26:5315-5336. doi: 10.1175/JCLI-D-12-00556.1

482 Liu Y, Lee S-K, Muhleng BA, Lamkin JT, Enfield DB (2012) Significant reduction of the Loop
483 Current in the 21st century and its impact on the Gulf of Mexico. *J Geophys Res* 117:
484 C05039. doi:10.1029/2011JC007555

485 Manabe S, Bryan K (1969) Climate calculations with a combined ocean-atmosphere model. *J*
486 *Atmos Sci* 26:786-789

487 Meehl G, Covey C, McAvaney B, Latif M, Stouffer R (2005) Overview of the coupled model
488 intercomparison project (CMIP). *Bull Amer Meteor Soc* 86:89-93

489 Mechoso CR, and coauthors (1995) The seasonal cycle over the tropical Pacific in coupled
490 ocean–atmosphere general circulation models. *Mon Wea Rev* 123:2825-2838

491 Neale RB, and coauthors (2010) Description of the NCAR Community Atmosphere Model
492 (CAM4.0). NCAR Tech Note 485+STR, 212 pp.

493 Okumura Y, Xie S-P (2004) Interaction of the Atlantic equatorial cold tongue and the African
494 monsoon. *J Clim* 17:3589–3602

495 Patricola CM, Chang P, Saravana R, Li M, Hsieh J-S (2011) An investigation of the tropical
496 Atlantic bias problem using a high-resolution coupled regional climate model. *US CLIVAR*
497 *Variations*, 9, U.S. CLIVAR Office, Washington, DC, 9-12. [Available online at
498 <http://www.usclivar.org/Newsletter/V9N2.pdf>.]

499 Richter I, Xie S-P (2008) On the origin of equatorial Atlantic biases in coupled general
500 circulation models. *Clim Dyn* 31:587-598

501 Richter I, Xie S-P, Wittenberg AT, Masumoto Y (2012) Tropical Atlantic biases and their
502 relation to surface wind stress and terrestrial precipitation. *Clim Dyn* 38:985–1001

503 Saha S, and coauthors (2006) The NCEP climate forecast system. *J Clim* 19:3483–3517. doi:
504 <http://dx.doi.org/10.1175/JCLI3812.1>

505 Seo H, Jochum M, Murtugudde R, Miller AJ (2006) Effect of ocean mesoscale variability on the
506 mean state of tropical Atlantic climate. *Geophys Res Lett* 33:L09606.
507 doi:10.1029/2005GL025651

508 Wahl S, Latif M, Park W, Keenlyside N (2011) On the tropical Atlantic SST warm bias in the
509 Kiel climate model. *Clim Dyn* 36:891-906

510 Wang C, Enfield DB, Lee S-K, Landsea CW (2006) Influences of the Atlantic warm pool on
511 Western Hemisphere summer rainfall and Atlantic hurricanes. *J Clim* 19:3011–3028. doi:
512 <http://dx.doi.org/10.1175/JCLI3770.1>

513 Wang C, Lee S-K (2007) Atlantic warm pool, Caribbean low-level jet, and their potential impact
514 on Atlantic hurricanes. *Geophys Res Lett* 34:L02703. doi:10.1029/2006GL028579

515 Webster PJ, Holland GJ, Curry JA, Chang H-R (2005) Changes in tropical cyclone number,
516 duration, and intensity in a warming environment. *Science* 309:1844-1846

517 Williams KD, and coauthors (2013) The Transpose-AMIP II experiment and its application to
518 the understanding of southern ocean cloud biases in climate models. *J Clim*, 26:3258–3274.
519 doi: <http://dx.doi.org/10.1175/JCLI-D-12-00429.1>

520 Vizy EK, Cook KH (2001) Mechanisms by which Gulf of Guinea and eastern North Atlantic sea
521 surface temperature anomalies can influence African rainfall. *J Clim* 14:795–821

522 Xie S-P, Carton JA (2004) Tropical Atlantic variability: Patterns, mechanisms, and impacts, in
523 *Earth's Climate: The Ocean-Atmosphere Interaction*, Geophys Monogr Ser vol. 147, edited
524 by Wang C, Xie S-P, Carton JA, pp. 121–142, AGU, Washington, D.C.,
525 doi:10.1029/147GM07

526 Yu JY, Mechoso CR (1999) Links between annual variations of Peruvian stratocumulus clouds
527 and of SST in the eastern equatorial Pacific. *J Clim* 12:3305-3318

528

529

530

531

532

533

534

535

536

537

538 **Figure captions**

539 **Figure 1.** Annually averaged climatological SSTs in the tropical Atlantic from (a) ERSSTv3 for
540 1949-2005, and (b) CCSM4 historical simulation for 1949-2005. The SST bias in CCSM4
541 (shaded) is also shown in (b). The unit is °C.

542

543 **Figure 2.** Annually averaged implicit SST bias in EXP_ATM due to (a) the net surface heat flux
544 bias, which is computed by integrating the net heat flux bias in EXP_ATM for one year from
545 January 1 to December 31, then dividing it by 12 months. Contributions by (b) shortwave
546 radiative heat flux bias, (c) latent heat flux bias and (d) longwave radiative heat flux bias. The
547 vectors in (c) show the annually averaged surface wind stress bias. The unit is °C.

548

549 **Figure 3.** Annually averaged SST bias in EXP_OCN. The unit is °C.

550

551 **Figure 4.** Annually averaged implicit SST bias in (a) EXP_OCN and (b) EXP_ATM +
552 EXP_OCN. (c) Annually averaged SST bias in EXP_CPL. The unit is °C.

553

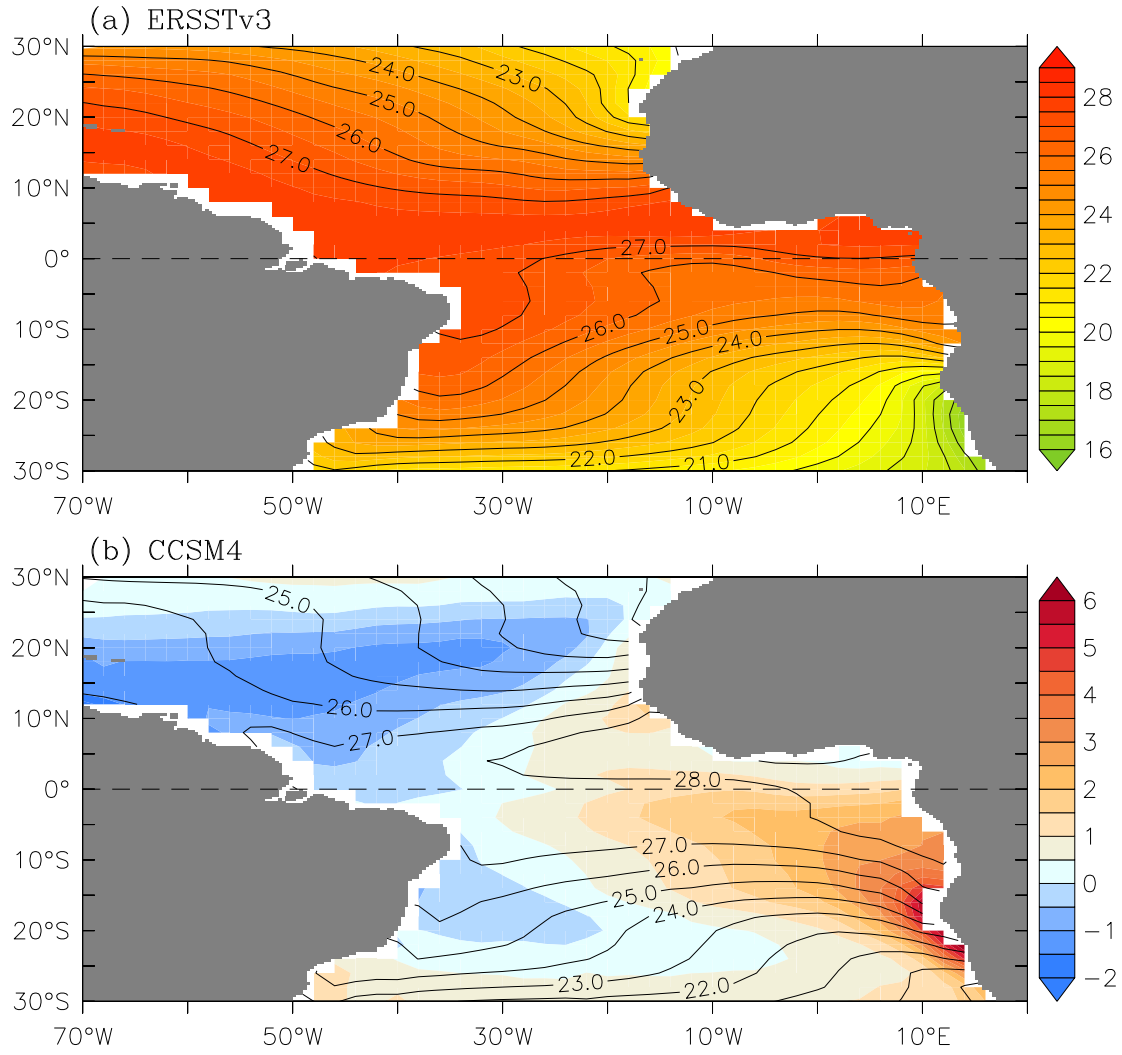
554 **Figure 5.** Evolution of SST bias in EXP_CPL during the first and second year. The unit is °C.

555

556 **Figure 6.** (1st column) Evolution of SST bias tendency in EXP_CPL during the first year.
557 Evolution of implicit SST bias tendency in (2nd column) EXP_ATM + EXP_OCN, (3rd column)
558 EXP_ATM, and (4th column) EXP_OCN. The unit is °C month⁻¹.

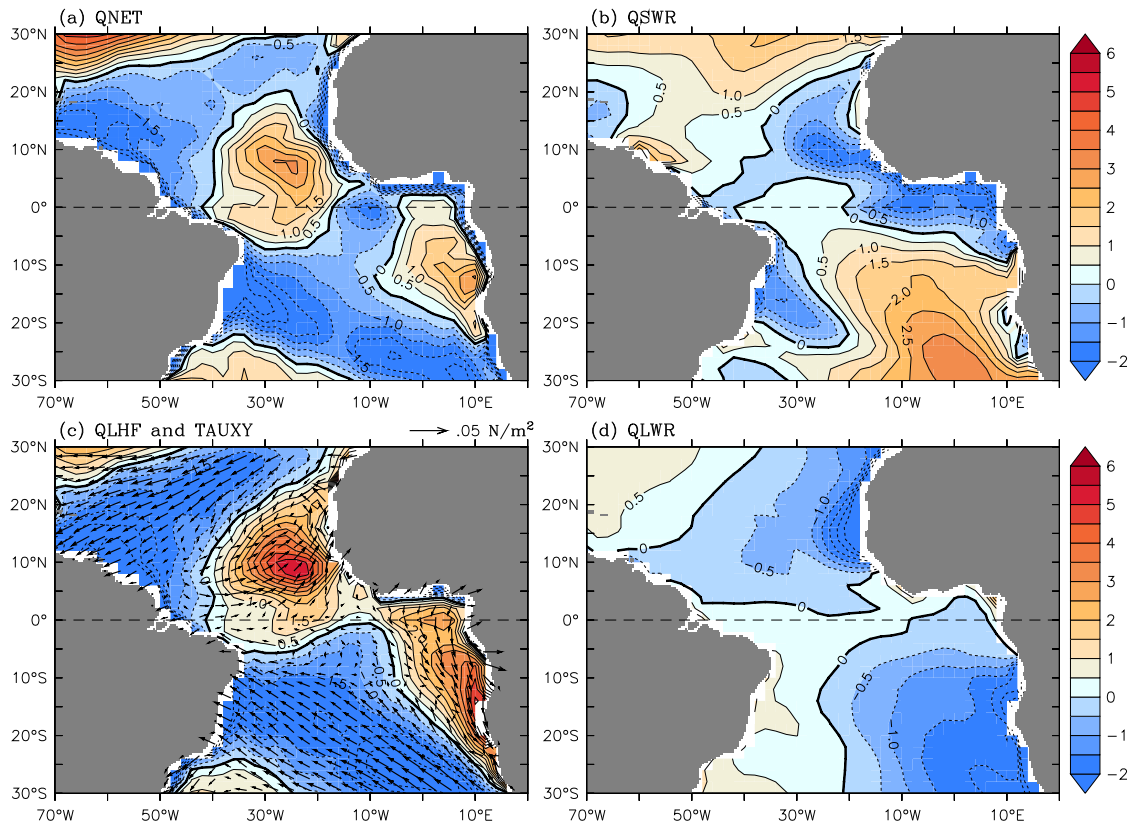
559

560 **Figure 7.** Time-longitude evolutions of (a) the SST bias tendencies along the equatorial Atlantic,
561 and the contributions by (b) the surface heat flux errors and (c) errors involving ocean dynamic
562 processes in EXP_CPL during the first year. Time-longitude evolutions of implicit SST bias
563 tendencies in (d) EXP_ATM + EXP_OCN, (e) EXP_ATM and (f) EXP_OCN. The unit is °C
564 month⁻¹.



1
 2 **Figure 1.** Annually averaged climatological SSTs in the tropical Atlantic from (a) ERSSTv3 for
 3 1949-2005, and (b) CCSM4 historical simulation for 1949-2005. The SST bias in CCSM4
 4 (shaded) is also shown in (b). The unit is °C.

5
 6
 7
 8



9

10 **Figure 2.** Annually averaged implicit SST bias in EXP_ATM due to (a) the net surface heat flux
 11 bias, which is computed by integrating the net heat flux bias in EXP_ATM for one year from
 12 January 1 to December 31, then dividing it by 12 months. Contributions by (b) shortwave
 13 radiative heat flux bias, (c) latent heat flux bias and (d) longwave radiative heat flux bias. The
 14 vectors in (c) show the annually averaged surface wind stress bias. The unit is °C.

15

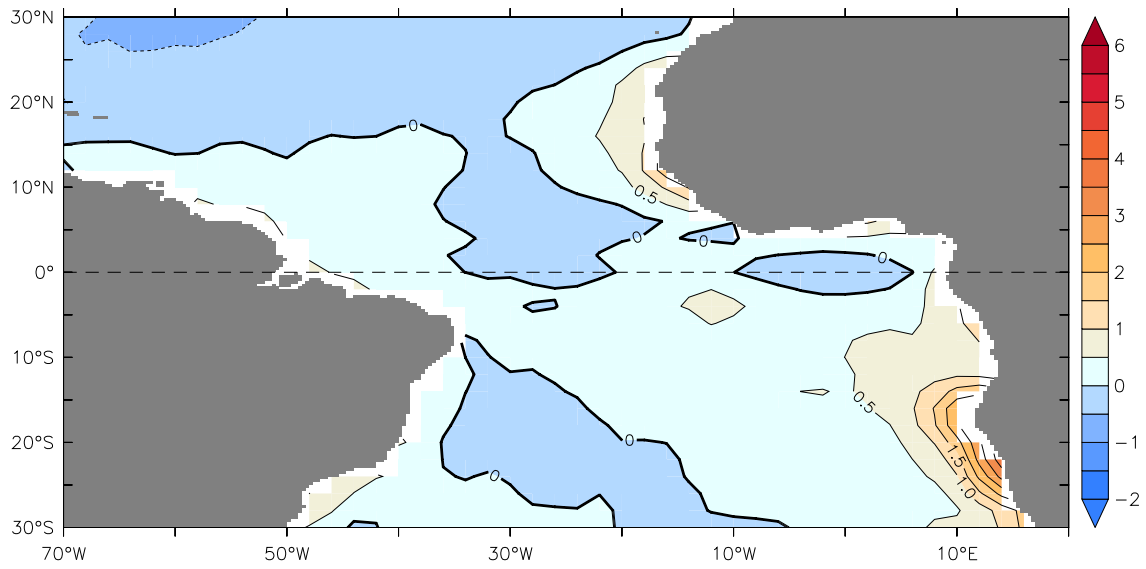
16

17

18

19

20



21

22 **Figure 3.** Annually averaged SST bias in EXP_OCN. The unit is °C.

23

24

25

26

27

28

29

30

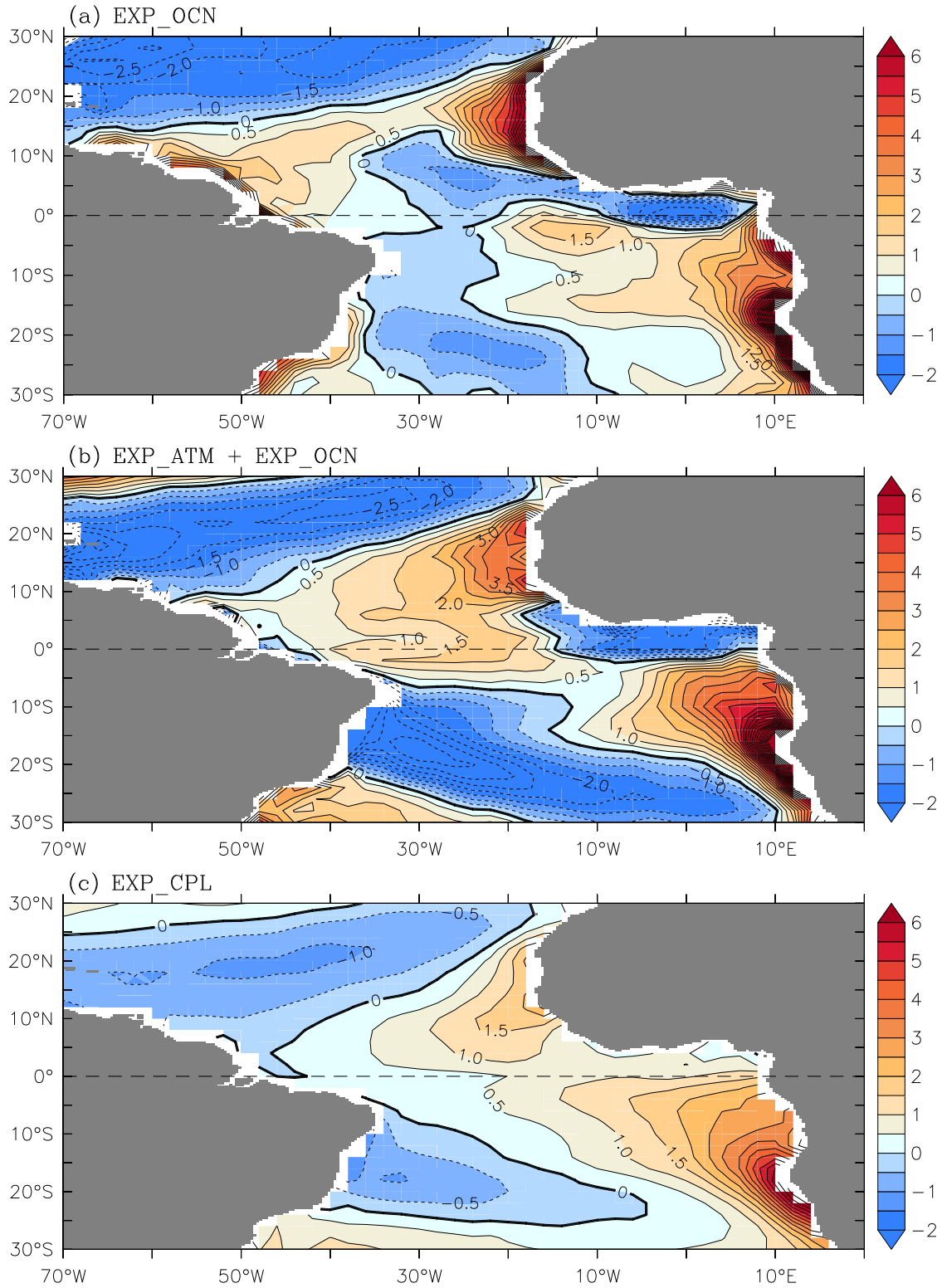
31

32

33

34

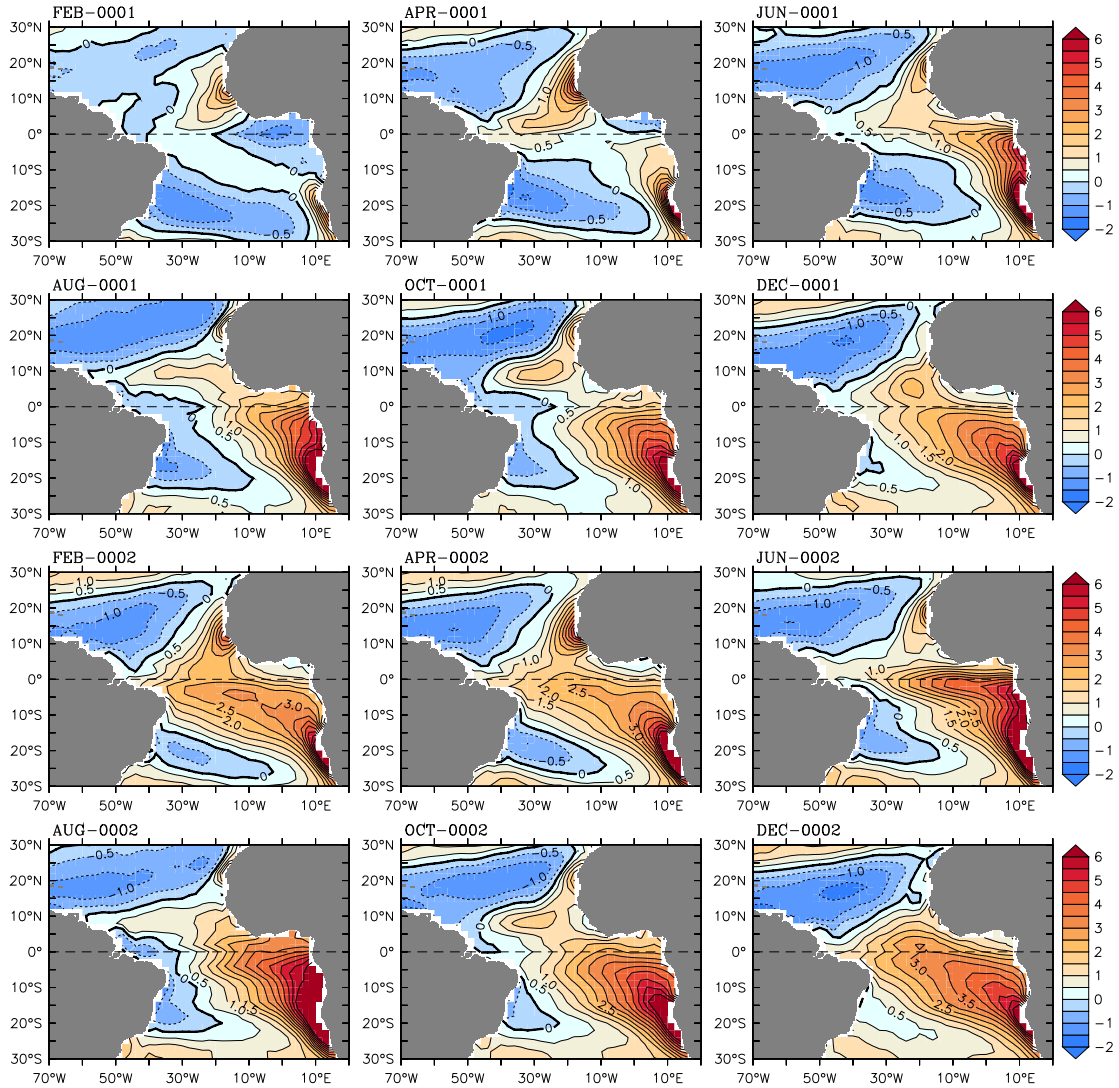
35



36

37 **Figure 4.** Annually averaged implicit SST bias in (a) EXP_OCN and (b) EXP_ATM +

38 EXP_OCN. (c) Annually averaged SST bias in EXP_CPL. The unit is °C.



39

40 **Figure 5.** Evolution of SST bias in EXP_CPL during the first and second year. The unit is $^{\circ}\text{C}$.

41

42

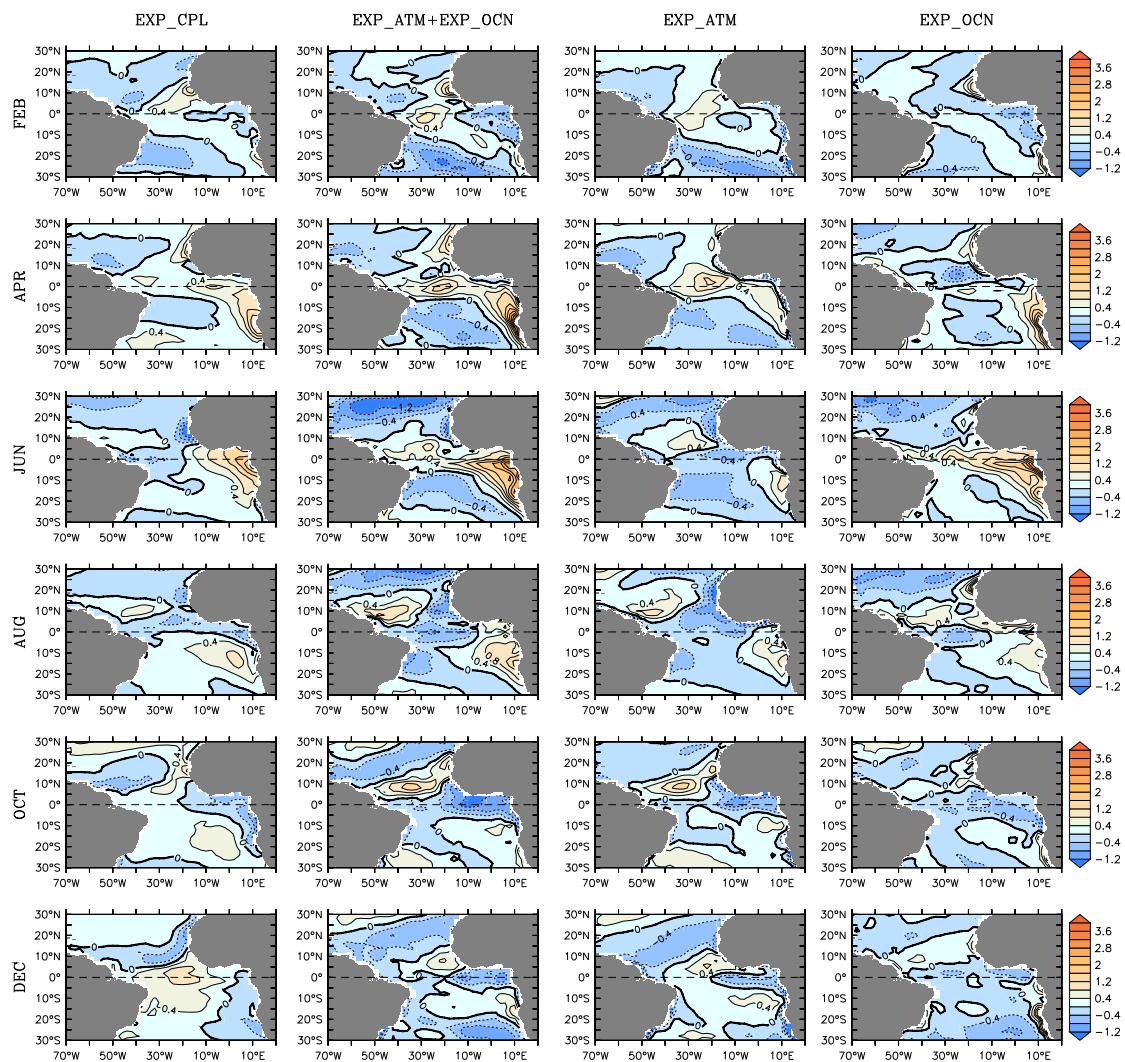
43

44

45

46

47



48

49 **Figure 6.** (1st column) Evolution of SST bias tendency in EXP_CPL during the first year.

50 Evolution of implicit SST bias tendency in (2nd column) EXP_ATM + EXP_OCN, (3rd column)

51 EXP_ATM, and (4th column) EXP_OCN. The unit is $^{\circ}\text{C month}^{-1}$.

52

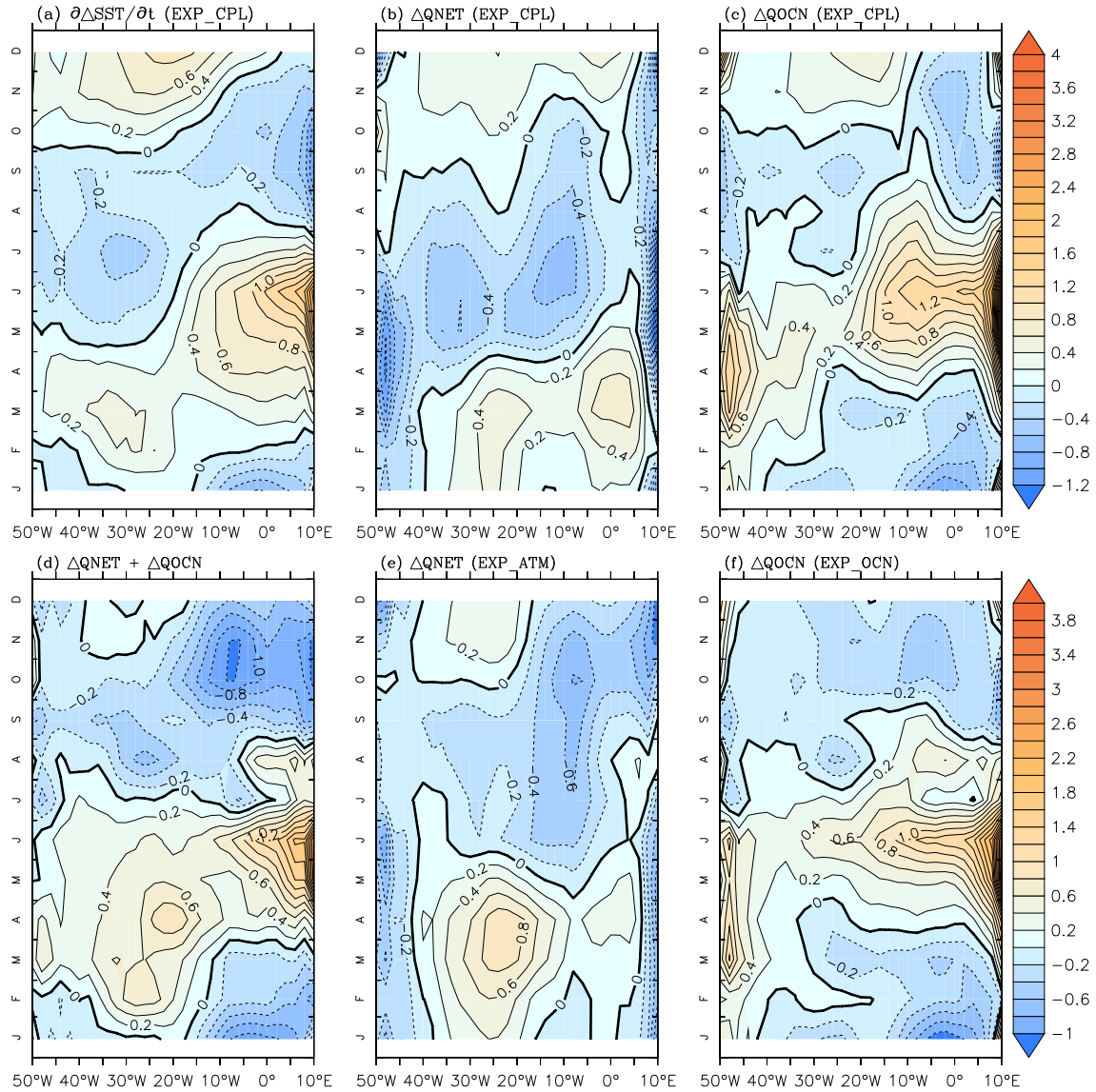
53

54

55

56

57



58

59 **Figure 7.** Time-longitude evolutions of (a) the SST bias tendencies along the equatorial Atlantic,

60 and the contributions by (b) the surface heat flux errors and (c) errors involving ocean dynamic

61 processes in EXP_CPL during the first year. Time-longitude evolutions of implicit SST bias

62 tendencies in (d) EXP_ATM + EXP_OCN, (e) EXP_ATM and (f) EXP_OCN. The unit is $^{\circ}\text{C}$

63 month^{-1} .